



NLR-TP-2015-275

Multi-level structural analysis for sub-component validation in aircraft composite fuselage structures

W.J. Vankan, W.M. van den Brink and R. Maas

Nationaal Lucht- en Ruimtevaartlaboratorium

National Aerospace Laboratory NLR

Anthony Fokkerweg 2

P.O. Box 90502

1006 BM Amsterdam

The Netherlands

Telephone +31 (0)88 511 31 13

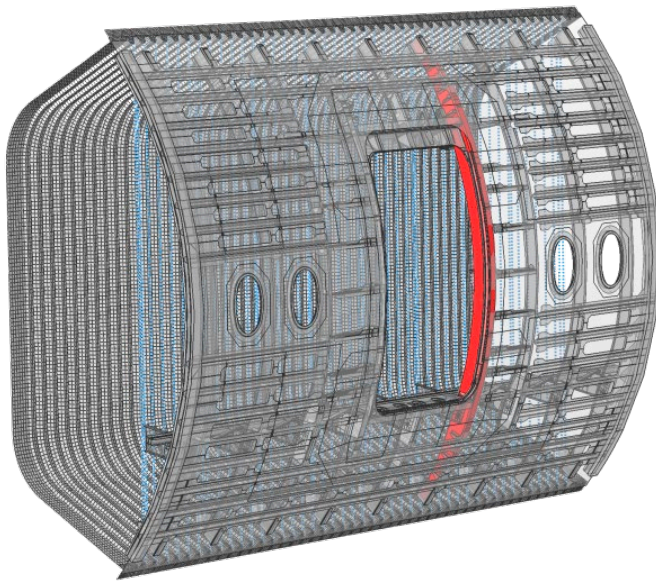
Fax +31 (0)88 511 32 10

www.nlr.nl



Executive summary

Multi-level structural analysis for sub-component validation in aircraft composite fuselage structures



The global FE model of the full-scale demonstrator test panel with the C72 door frame sub-component indicated in red

Report no.

NLR-TP-2015-275

Author(s)

W.J. Vankan
W.M. van den Brink
R. Maas

Report classification

UNCLASSIFIED

Date

January 2016

Knowledge area(s)

Computational Mechanics and
Simulation Technology

Descriptor(s)

panel test
CAD
finite element model
load identification
damage simulation

Problem area

NLR participates in the MAAXIMUS project (More Affordable Aircraft structure through eXtended, Integrated & Mature nUmerical Sizing) to develop capabilities for the fast development and right-first-time validation of a highly-optimized composite airframe. This is achieved through co-ordinated developments on a physical platform, by developing and validating the appropriate

composite technologies for low weight aircraft, and on a virtual platform, to identify faster and validate earlier the best solutions.

One of the investigations in MAAXIMUS deals with the reduction of time and costs needed for full-scale structural validation testing, which is usually done on fuselage barrel level. The aim is to achieve validation testing on a slightly lower level of the test pyramid, for example on large

This report is based on a presentation held at the EUCASS 2015 Conference, Krakow, Poland, 29 June - 3 July 2015.

fuselage panels that do include the critical and complex structural features of the aircraft fuselage.

Description of work

The present paper describes a finite element test modelling study (virtual testing) of a large composite fuselage side panel with substantial structural details like frames, stringers, floor beams, windows and door surround structures. The focus of this study is to support the development of the innovative physical test set-up through detailed modelling of the test-sample including the relevant aspects of the test-rig. Proper loads and boundary conditions from the test rig are incorporated and the global structural response is evaluated. Local structural responses in sub-components like frames are evaluated in high detail using ABAQUS sub-modelling to accurately capture local stress states during tests and to evaluate local failures in these components. A small explorative study is presented that investigates local strain effects in the test around an impact damage location in one frame. This small study illustrates the applicability of this approach for demonstrating that such damaged areas remain stable during the test campaign (virtual assessment of no-growth principle).

Results and conclusions

For the virtual test of the side panel, detailed finite element models (DFEMs) of the side panel and of the fuselage barrel are used. The panel DFEM assembly is derived from a detailed CAD model. For the proper determination of the load values to be applied in the panel DFEM, an identification study of the panel loads is performed through data correlation of the strain fields occurring in the panel and in the barrel DFEMs. The sub-modelling approach is used to evaluate in high detail the localised region around damage locations. Various levels of damage modelling are applied for accurate prediction of progression from inflicted category 1 and 2 impact damages. It is demonstrated that these damages can be expected to remain stable during the test campaign.

Applicability

The virtual testing approach used here can be applied to any large scale structural validation test, i.e. not only fuselage but any primary aircraft structure. The damage evaluation analysis presented here applies specifically to composite structures, but the overall virtual testing approach is also applicable to metallic structures.



NLR-TP-2015-275

Multi-level structural analysis for sub-component validation in aircraft composite fuselage structures




W.J. Vankan, W.M. van den Brink and R. Maas

This report is based on a presentation held at the EUCASS 2015 Conference, Krakow, Poland, 29 June – 3 July 2015.

The contents of this report may be cited on condition that full credit is given to NLR and the authors. This publication has been refereed by the Advisory Committee AEROSPACE VEHICLES.

Customer National Aerospace Laboratory NLR
Contract number ---
Owner NLR
Division NLR Aerospace Vehicles
Distribution Unlimited
Classification of title Unclassified
January 2016

Approved by:

Author W.J. Vankan 	Reviewer B.A.T. Noordman 	Managing department A.A. ten Dam 
Date: 20-1-2016	Date: 27-01-2016	Date: 01-02-2016

Contents

Abstract	3
1. Introduction	3
2. Modelling Approach	6
3. Panel design and CAD model assembly	6
4. Panel DFEM for virtual testing	7
5. Loads identification / Data correlation, global structure response	8
6. Sub-modelling	9
7. Damage analyses	11
8. Global conclusions and discussion	14
References	15
Acknowledgements	15

Multi-level structural analysis for sub-component validation in aircraft composite fuselage structures

W.J. Vankan, W.M. van den Brink* and R. Maas**

**Dept. Collaborative Engineering Systems, Aerospace Vehicles Division, National Aerospace Laboratory NLR, Anthony Fokkerweg 2, 1059 CM Amsterdam, the Netherlands; jos.vankan@nlr.nl*

Abstract

The present paper describes a finite element test modelling study (virtual testing) of a large composite fuselage side panel with substantial structural details like frames, stringers, floor beams, windows and door surround structures. Proper loads and boundary conditions from the test rig are incorporated and the global structural response is evaluated. Local structural responses in sub-components like frames are evaluated in high detail using sub-modelling to accurately capture local stress states during tests and to evaluate local failures in these components, e.g. related to manufacturing defects or damages, to demonstrate that these failures remain stable during the test campaign (virtual assessment of no-growth principle).

1. Introduction

In composite aircraft fuselage development, validation of new composite design and material technologies is ultimately done by full-scale testing on fuselage barrel level. However, to reduce time and costs needed for such tests, this full-scale validation is aimed to be done on a slightly lower level of the test pyramid, for example on large fuselage panels that do include the critical and complex structural features as for example circumferential or longitudinal joints, PAX door and the corresponding door surround structure or representative floor structures.

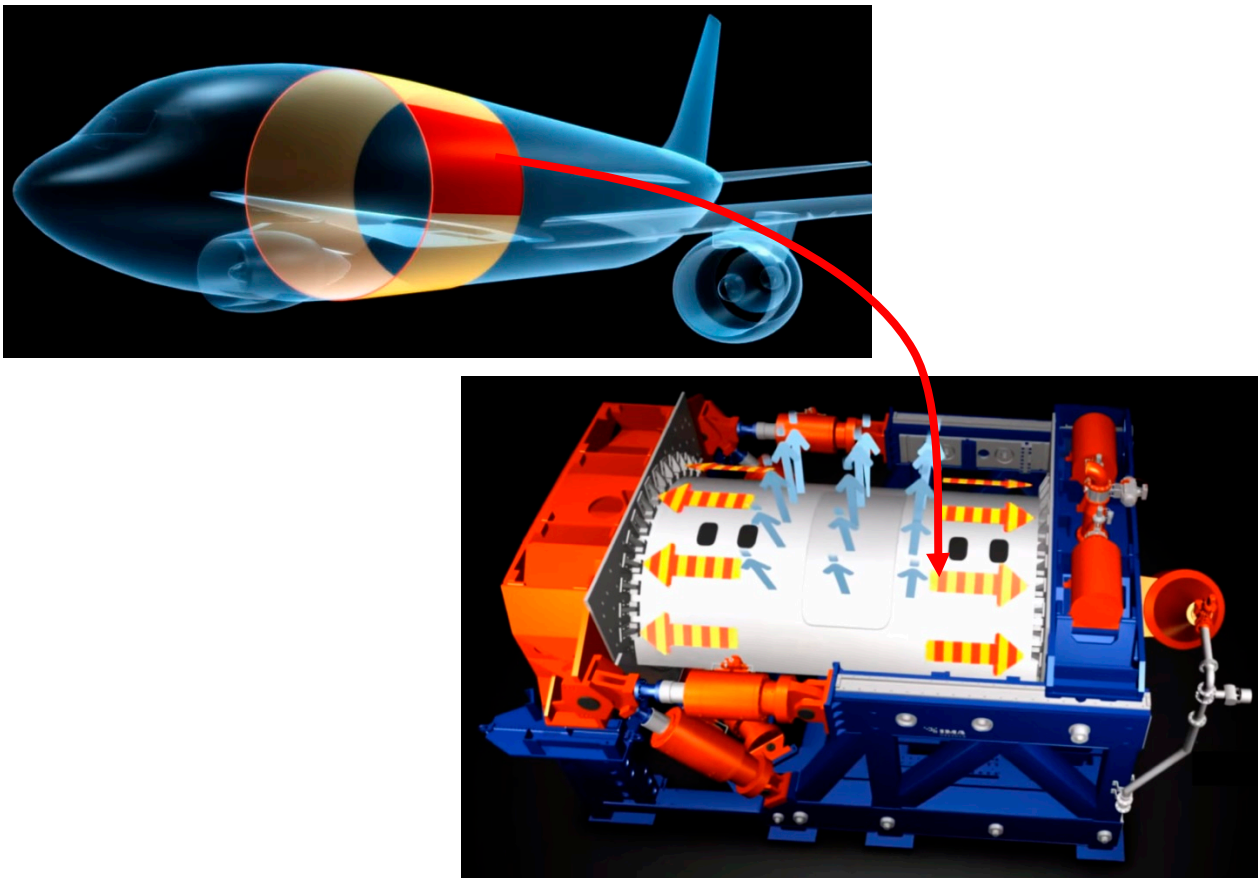


Figure 1 Illustration of aircraft front-fuselage barrel (upper figure), and panel cut-out being tested in a large fuselage panel test rig (lower figure) as developed at IMA [2].

Such tests require quite advanced and complex test rigs with sufficient flexibility to accurately impose the required loads and boundary conditions on the considered test article: proper load introduction of shear and bending loads, airtight sealing to allow for pressurisation loading, correct fixation and loading of stringers, frames and floor beams. Such advanced test rigs have been developed in the past, for example for metallic narrow-body aircraft [1], and have been further developed for larger panels and for improved versatility in loading and test conditions, e.g. [2] (see Figure 1).

One of the main performance criteria for such advanced panel level test rigs is to introduce loads into the test article in such a way that the structural response in the test rig is fully consistent with the full-scale testing on fuselage barrel level, which is as close as possible to the in-flight situation. To capture the behaviour of the structure in the full-scale barrel test, accurate modelling and analyses of the detailed behaviour of the barrel structure are applied. This is typically achieved through extensive model studies (“virtual testing”) using large finite element (FE) models [4], for example highly detailed models of aircraft fuselage structures Figure 2.

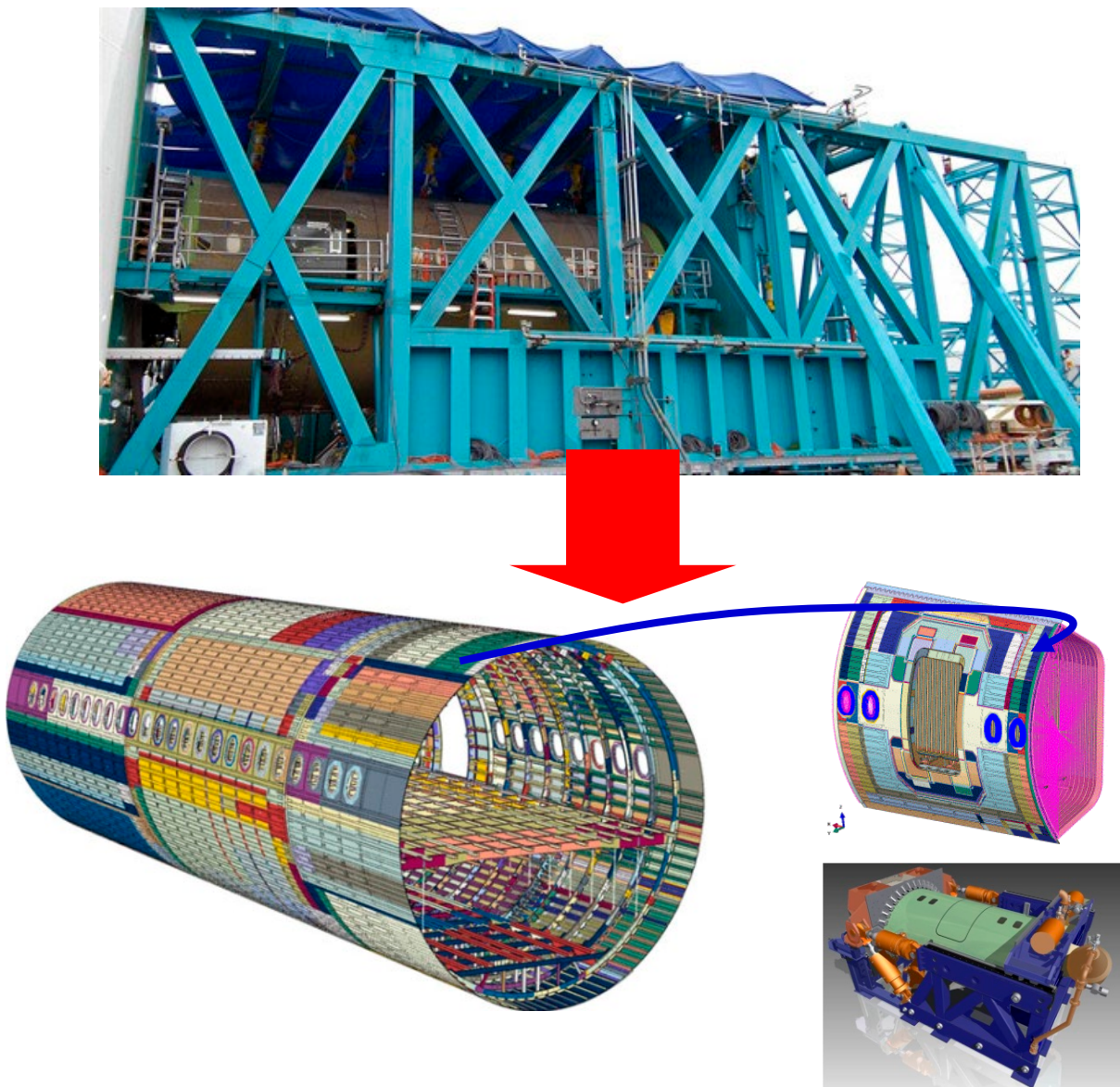


Figure 2 Full-scale barrel physical testing, as applied for example to Boeing 787 fuselage [3] (upper picture), to be replaced by large panel physical testing accompanied by barrel and panel level virtual testing (lower pictures). Highly detailed FE models of aircraft fuselage barrel structure (lower left) are used in virtual testing studies at Airbus [4] for virtual representation of full-scale barrel tests, thus enabling realistic large panel level virtual testing (upper right) and physical testing [2] (lower right).

Furthermore, the tests with such advanced panel level test rigs can include the evaluation of structural repairs and representative damages inflicted to the test article for fail-safe and damage tolerance testing. For example for category 1 impact damages (BVID manufacturing defects) the structure is required to sustain ultimate load design load levels as defined by the American Federal Aviation Administration (FAA) Advisories, see Figure 3 below. For the Category 2 damages (VID) a sufficient margin above limit load is advised.

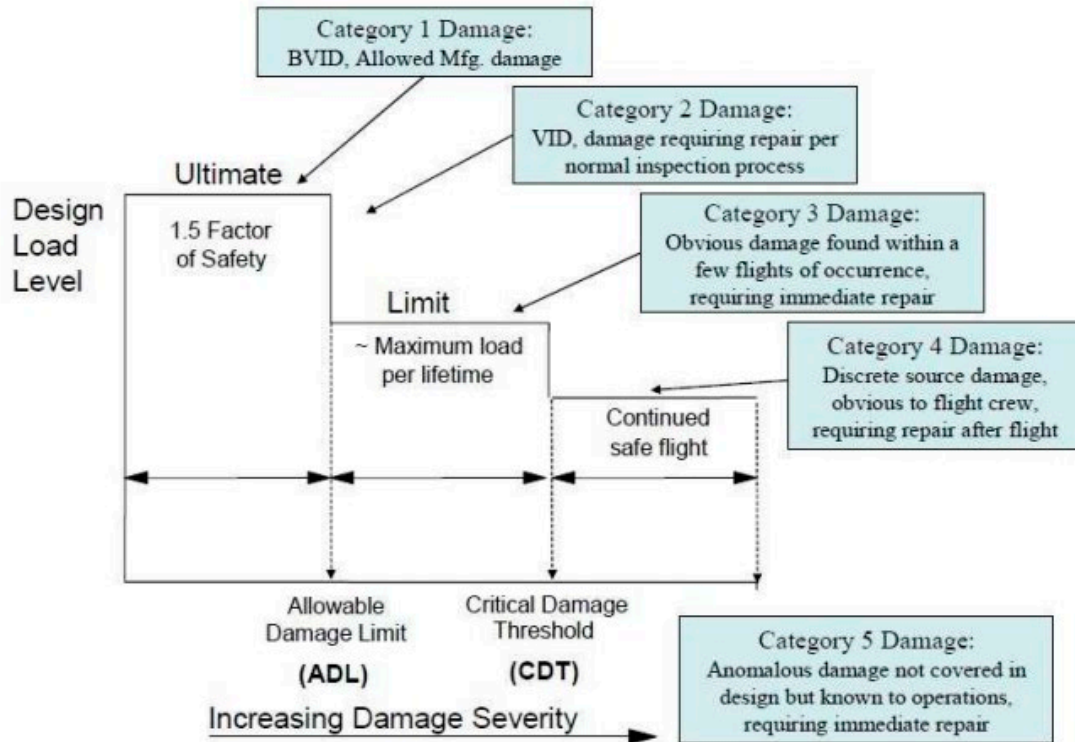


Figure 3 Design load levels versus categories of damage severity [7].

To capture the global response of the test article, as well as the detailed local responses in vicinity of repairs and damages, test results are obtained from a variety of sensors like local strain gauges and global deformation and strain measurements with optical measurement technology (using digital image correlation DIC). Because of the complexity of these tests and the richness of test data that are produced, also on this level the accurate modelling and analyses of the detailed behaviour of the test article through “virtual testing” are applied. These detailed FE models can be used for the design of the interfaces between the test article and the test rig, but also for the analysis of critical localised phenomena such as stress or strain concentrations, identification of hotspots for damage infliction, damage initiation and propagation.

The present paper deals with a virtual testing study of a large composite fuselage side panel with substantial structural details like stringers, frames, floor beams and PAX door and windows with their surrounding stiffening structures. The focus of this study is to support the development of the innovative physical test set-up through detailed modelling of the test-sample including the relevant aspects of the test-rig. Proper loads and boundary conditions for the test rig are determined and the global structural response of the side panel is evaluated. An identification study is presented using the barrel and panel strains for the proper determination of the load values to be applied in the physical test procedure. From the global structural response, local structural responses in sub-components like stringers and frames are evaluated in high detail using ABAQUS sub-modelling in order to accurately capture their load state in the test and to identify possibly local failures in these components, e.g. related to small manufacturing defects. The sub-modelling approach can also be used to evaluate in high detail the localised region around damage locations and various levels of damage modelling can be applied, e.g. for accurate prediction of progression from inflicted category 1 and 2 impact damages. A small explorative study is presented that investigates local strain effects in the test around an impact damage location in one frame. This small study illustrates the applicability of this approach for demonstrating that such damaged areas remain stable during the test campaign (virtual assessment of no-growth principle).

The experimental validation of the virtual tests analyses results obtained in this study is beyond the scope of this paper because the physical test evaluation of the side panel has not yet been executed at the time of the paper's publication.

The work presented in this paper has been performed in co-operation with partners in the EU FP-7 project MAAXIMUS [8].

2. Modelling Approach

For the virtual test of the side panel, detailed finite element models (DFEMs) of the side panel and of the fuselage barrel are needed. In this paper the focus will be mainly on the development and the analyses of the panel DFEM; the modelling details of the barrel DFEM are comparable to those of the panel.

The panel model is based on the panel design as given by a detailed CAD model. The panel DFEM assembly is derived from the detailed CAD model, mainly for its geometry, assembly and properties. Also the systems for introduction of the loads from the test rig (force/moment actuators, internal pressure) are included in the panel DFEM and loads and boundary conditions are prescribed.

For the proper determination of the load values to be applied in the panel DFEM, an identification study of the panel loads is performed through data correlation of the strain fields occurring in the panel and in the barrel DFEMs.

Initially, analyses on the overall response of the panel DFEM are performed and stress and strain fields are calculated. For critical areas in the panel structure the sub-modelling approach is used to further detail these critical regions and to locally improve the fidelity of the analyses.

For further correlation and validation a comparison with the panel's physical test is foreseen but this is considered as future work and is not part of this paper.

3. Panel design and CAD model assembly

The design of the panel is consistent with the fuselage barrel design, i.e. all aspects and properties like diameter, curvature, skin thicknesses, frames, stringers, pitches, windows, floor structures, composite layups and materials are the same in the panel and the barrel models. The panel design is fully defined in a CATIA V5 [5] CAD model. It includes the above mentioned aspects and properties and all the details of its sub-structures and parts (see Figure 4) and consists of nine frame sections with an overall length of around 6 meters. For integration into the test rig, the panel is devised with several reinforcements and attachment structures at its free edges, door surrounds and floor beams to allow for proper load introductions.

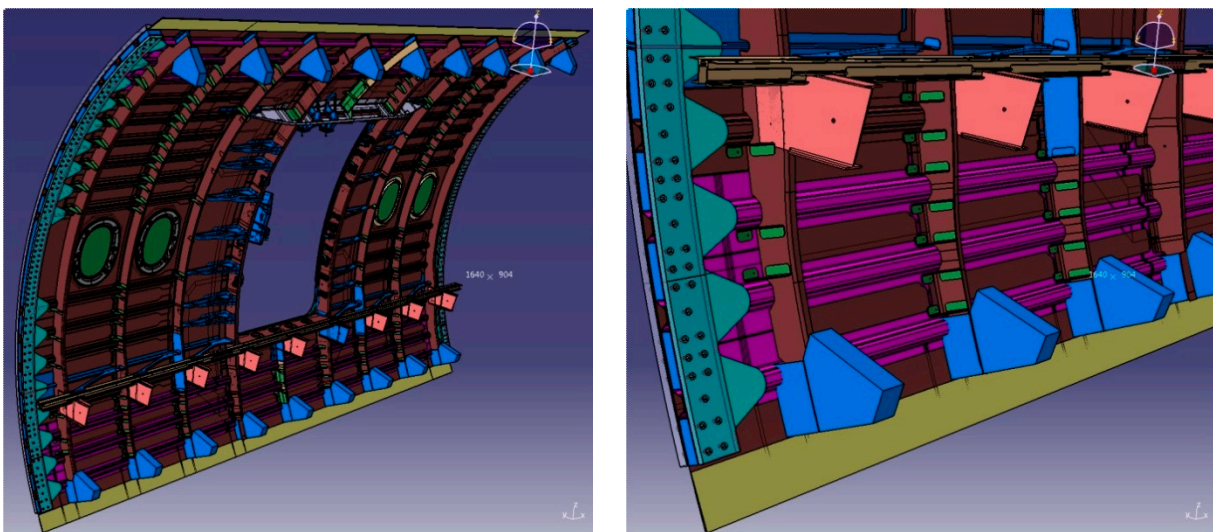


Figure 4 CAD model of the panel, including all the details of its sub-structures and parts, and reinforcements and attachment structures at its free edges to allow for proper load introductions (left). On the right a local view is given of the panel corner showing some of the modelling detail of the skin reinforcement structures at the curved edge.

It should be noted that the panel CAD does not include the PAX door. Because the door does not (or hardly) contribute to the in-plane stiffness of the fuselage, a detailed representation is not essential for the panel DFEM.

The detailed representation of the panel structure in the CAD model is adopted in the DFEM, but some of the small details are not essential for the analysis and therefore several simplifications are applied in the DFEM modelling process.

4. Panel DFEM for virtual testing

The detailed definitions of the panel structure in the CAD model are based on 3D solid representation in order to achieve sufficiently accurate representation and positioning in the CAD model assembly. Because virtually all parts in the panel are thin-walled structures, the DFEM of the panel is simplified to the mid-surface shell representation of nearly all parts. In particular the shell representation instead of solid representation of the large thin structures like skin, stringers and frames contribute to the reduction of model size.

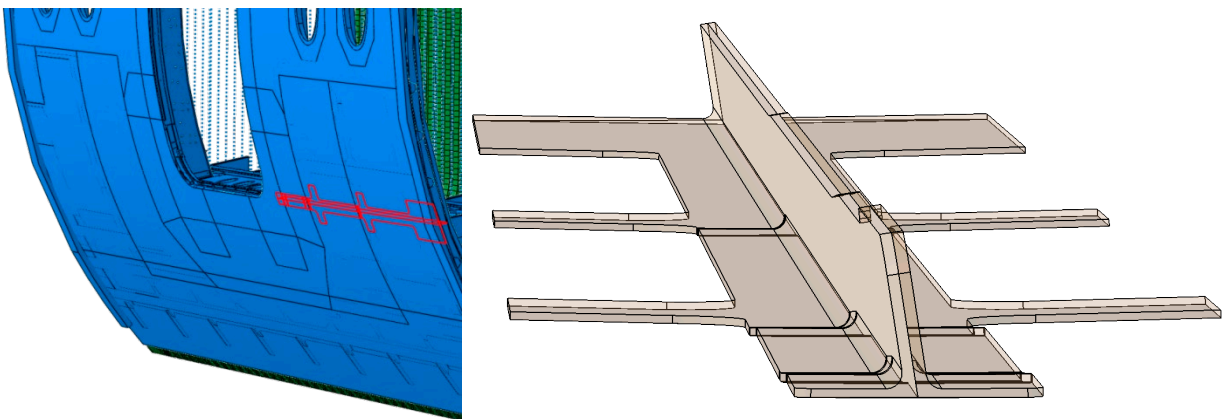


Figure 5 Example of the simplification of a T-stringer part from solid representation as defined in the CAD to its mid-surface shell representation in the DFEM.

Some further simplifications and de-featurings are applied in the CAD to DFEM transfer, for example by removing some small holes and some less significant parts (like some individual nuts and bolts). The DFEM is developed in the FE software ABAQUS [6], which offers specific functions, like mid-surface identification tools, to efficiently implement these simplifications. All the resulting parts (about 250) in the DFEM are properly positioned in the assembly and connected together with tie constraints; also for simplification, discrete fastener connections have not been applied in the DFEM. All parts' properties (like materials, composite layups) are adopted from the CAD model as far as available and parts are meshed (mostly) with linear shell elements yielding a total mesh of about 670k elements for the full DFEM assembly (see Figure 6).

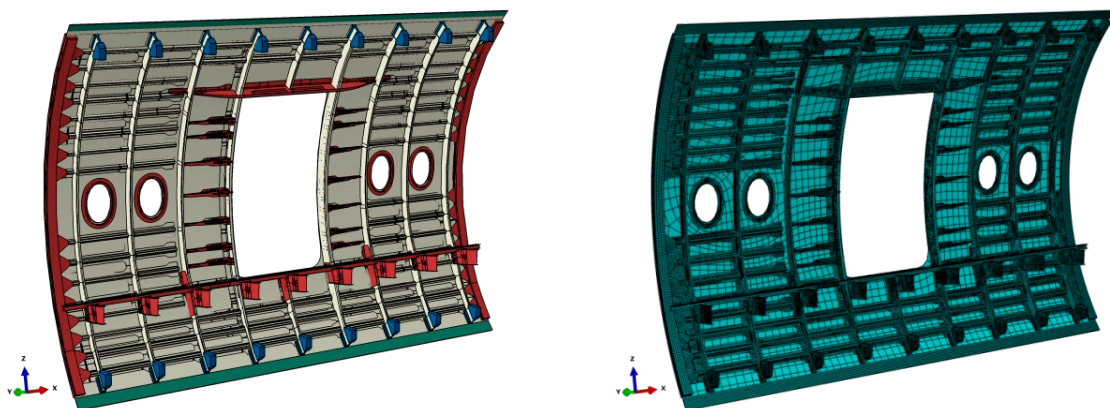


Figure 6 All approximately 250 parts are properly positioned in the DFEM assembly (left) and connected together with tie constraints. All parts are meshed (mostly) with linear shell elements yielding a total mesh of about 670k elements for the full DFEM assembly (right).

In addition to the FE model of the panel, also the relevant aspects of the test rig shall be properly incorporated in the panel DFEM. This mainly concerns the panel fixation and load introduction into the panel, for which several reinforcements and attachment structures at the panel's free edges are included. The main loads are introduced at the panel's edges and at the cross-beams' ends. Additional forces and moments at the straight skin edges and frame-ends are introduced by so-called skin- and frame-spreaders, and are applied for compensation of the stiffness of the barrel structures that would surround the panel. Furthermore the installation for pressurisation, which is achieved by a so-called pressure box that has sufficient pressure stiffness but relatively low bending and torsion stiffness, is included in the DFEM.

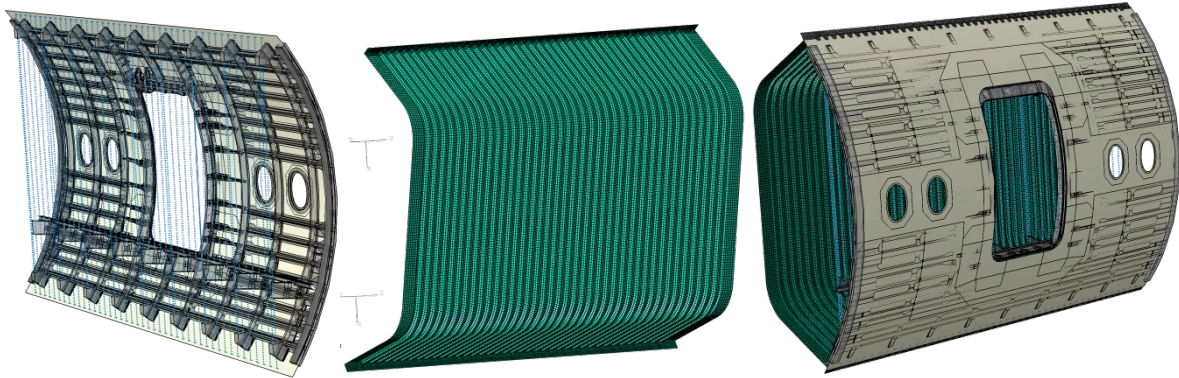


Figure 7 Integration of the main load introduction components in the panel DFEM. Left picture: skin-spreaders (vertical lines between the upper and lower edges of the panel) are modelled as discrete connectors between which forces can be actuated; frame-spreaders are modelled similarly between the upper and lower ends of the frames. Middle picture: the pressure box is modelled as a relatively flexible shell structure. Right picture: the full DFEM assembly after the incorporation of spreaders and pressure box.

The overall construction of the test rig (see Figure 1), consisting of its steel frame structure, actuators and grips, has much higher stiffness than the panel and is therefore assumed rigid and incorporated in the DFEM as boundary conditions and constraints. Because the PAX door does not contribute to the in-plane stiffness of the fuselage, it will be represented in the model in a simplified way. For similar reasons the windows are incorporated in a simplified way in the panel DFEM. Consequently the in-plane stiffness is neglected for the PAX door and window cut-outs, and out-of-plane loads due to pressurisation are included as distributed loads on the the door-stops and cut-outs edges. The resulting DFEM of the panel, including the relevant structures for pressurisation and load introduction, is shown in Figure 7.

5. Loads identification / Data correlation, global structure response

The loads in the panel are applied by the test rig through an extensive set of hydraulic actuators and a pneumatic pressurisation system. These loads shall represent the load distribution from barrel-level load-cases such as lateral bending, vertical bending and internal pressure. In the test rig a total of 21 independent load signals are used, each signal controlling one or several of the hydraulic actuators and one signal controlling the pneumatic pressurisation of the panel. Some of the large external hydraulic actuators of the test rig (see Figure 1) deliver the concentrated forces and moments as applied to the panel's loaded edge (one of the curved edges is effectively loaded by 3 independent forces and 3 independent moments; the other curved edge is fixed). Many other hydraulic actuators, mounted internally in the pressure box, deliver the forces and moments on cross-beams, frame-spreaders and skin-spreaders.

The 21 load signals shall be determined such that the deformation of the panel in the test rig is as close as possible to the deformation that would occur in the full-scale barrel test for a given load-case (for example, a lateral bending left (LBL) case). Therefore the barrel DFEM can be used to simulate the deformation that would occur in the full-scale barrel test. From the barrel simulations, large sets of surface strain data (typically including ϵ_{11} , ϵ_{12} , ϵ_{22}) in the panel region of the barrel DFEM can be extracted that are representative for the strains in this region in the full-scale barrel test. Then the 21 independent load signals in the panel DFEM are tuned such that the surface strains in the panel are accurately matched to the strains from the barrel model. A least squares minimisation procedure, minimising the sum of squares of the residuals between the strains in the panel and the barrel, is applied to identify the load signals values that best match these strains. For efficiency of the minimisation procedure the superposition principle is applied and therefore the strains coming from linear panel DFEM analyses responses for pre-defined unit-load values for each of the 21 independent load signals are used. Hence linear unit-load analyses are performed for all 21 load signals

separately. The resulting $(\epsilon_{11}, \epsilon_{12}, \epsilon_{22})$ strain responses are collected in all strain locations and are stored in a 21 column-matrix. The least squares procedure determines the linear combination of these columns, i.e. the set of 21 load factors α , that yields the best approximation of the barrel strains, and is expressed in equation 1.

$$\min_{\alpha} \|\epsilon^b - \epsilon^p \alpha\|^2 \rightarrow \alpha = (\epsilon^{pT} \epsilon^p)^{-1} \epsilon^{pT} \epsilon^b \quad (1)$$

Where ϵ^p is the matrix with panel strain values for each of the 21 linear unit-load analyses and ϵ^{pT} is its transpose, ϵ^b is the matrix with the intended barrel strain values, and α is the column with the 21 load factors:

$$\epsilon^p = \begin{bmatrix} \epsilon_{11}^{1,1} & \epsilon_{11}^{1,2} & \dots & \epsilon_{11}^{1,21} \\ \vdots & \vdots & & \vdots \\ \epsilon_{11}^{n,1} & \epsilon_{11}^{n,2} & \dots & \epsilon_{11}^{n,21} \\ \epsilon_{12}^{1,1} & \epsilon_{12}^{1,2} & \dots & \epsilon_{12}^{1,21} \\ \vdots & \vdots & & \vdots \\ \epsilon_{12}^{n,1} & \epsilon_{12}^{n,2} & \dots & \epsilon_{12}^{n,21} \\ \epsilon_{22}^{1,1} & \epsilon_{22}^{1,2} & \dots & \epsilon_{22}^{1,21} \\ \vdots & \vdots & & \vdots \\ \epsilon_{22}^{n,1} & \epsilon_{22}^{n,2} & \dots & \epsilon_{22}^{n,21} \end{bmatrix}; \alpha = \begin{bmatrix} a_1 \\ a_2 \\ \vdots \\ a_{21} \end{bmatrix}; \epsilon^b = \begin{bmatrix} \epsilon_{11}^{1,barrel} \\ \vdots \\ \epsilon_{11}^{n,barrel} \\ \epsilon_{12}^{1,barrel} \\ \vdots \\ \epsilon_{12}^{n,barrel} \\ \epsilon_{22}^{1,barrel} \\ \vdots \\ \epsilon_{22}^{n,barrel} \end{bmatrix} \quad (2)$$

As a validation of the resulting values of these 21 load factors, the strains coming from non-linear analyses of the load-case resulting from the combined 21 load factors for the panel DFEM and the strains coming from non-linear analyses of the barrel DFEM are compared. This procedure can be executed for each of the considered load-cases, including for example vertical and lateral bending and pressurisation. In the present paper we focus on the unpressurized lateral bending left (LBL) limit load case, but other load cases (like pressurized vertical bending down) are treated in a similar way.

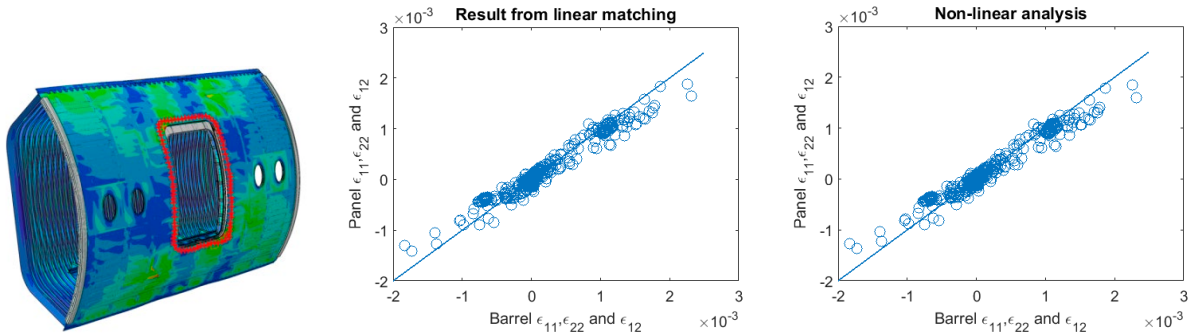


Figure 8 Illustration of the matching of strains coming from panel DFEM and barrel DFEM analyses. One sub-set of surface strain locations (at skin surface around the PAX door cut-out) is indicated in the panel DFEM (left picture). It should be noted that multiple sets of such strain locations are used in the loads identification procedure. The correlation plots of the strains from the panel DFEM versus the barrel DFEM, as obtained by least squares minimisation for one of the bending load-cases, are shown in the graphs (horizontal axis: barrel strains; vertical axis: panel strains; middle graph: strains from linear DFEM analyses; right graph: strains from non-linear DFEM analyses). Apparently the strains from the non-linear DFEM analyses are quite close to the strains from the linear DFEM analyses.

The strain levels in the DFEM model are compared with the reference case on the barrel level. Global reserve factors calculations for the possible failures that may occur in the tests, like damage propagation, buckling etc, can be subsequently performed with the panel DFEM.

6. Sub-modelling

The DFEMs of the barrel and the panel can be used for the test rig loads identification and for the design (sizing) of the interfaces (reinforcements and load introductions) between the test article and the test rig. But the panel DFEM can also be used for the analysis of critical localised phenomena that may occur during the tests such as stress or strain concentrations, identification of hotspots for damage infliction, damage initiation and propagation using advanced damage models.

From the global structural response of the panel DFEM, local structural responses (displacements) in sub-components like composite stringers and composite frames are evaluated in high detail using sub-modelling. This sub-modelling approach allows to accurately capture the load state of these components in the test and to identify possibly local failures in these components, e.g. related to small manufacturing defects. For the whole panel DFEM only a limited level of mesh detail is allowable for efficient calculation, i.e. only relatively coarse meshes on all the parts are used. A sub-model only represents a local region of the panel, e.g. a single part, and therefore allows for much smaller element sizes and still yielding efficient calculation of the specific region. The global structural response is transferred from the panel DFEM to the local region via prescribed displacements on the sub-model boundaries (i.e. only one-way coupling). Since the boundary conditions for the sub-model are automatically applied, the main difference between the sub-model and the panel DFEM is the mesh size and detailed connections, e.g. fasteners instead of ties.

Automated procedures in ABAQUS for assigning sub-modelling regions in FE models have been developed within the MAAXIMUS project [8] and are deployed in this work. Several hotspot areas have been detected in the panel DFEM at the door surround structure and window frames. These areas are considered for the sub-model approach. In this study the sub-modelling approach has been used to evaluate in high detail the localised region around damage locations and various levels of damage modelling are applied for accurate prediction of progression from inflicted category 1 and 2 impact damages. The purpose is to demonstrate that these damages can be expected to remain stable during the test campaign (virtual assessment of no-growth principle).

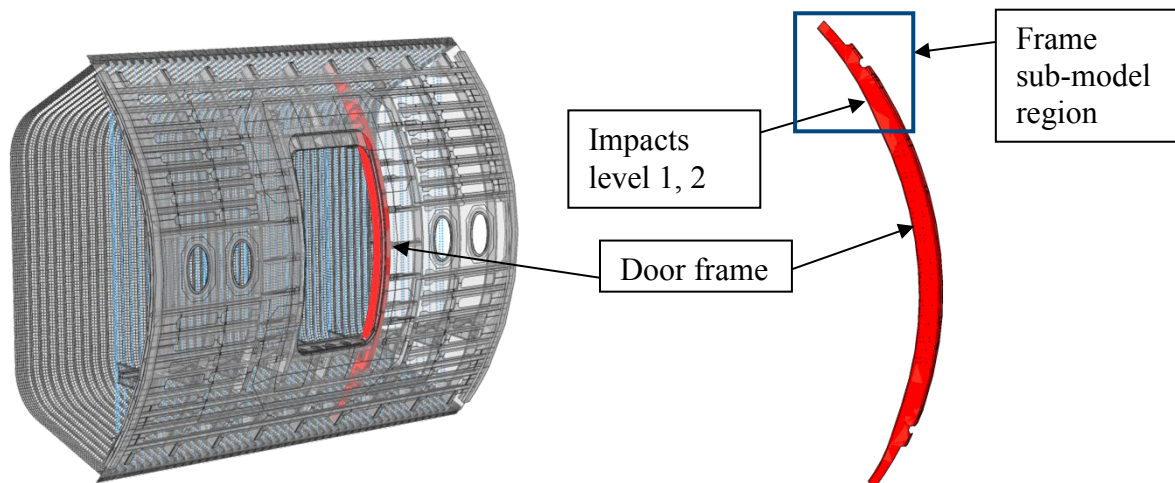


Figure 9 Global model of full scale demonstrator and subcomponent door frame C72 indicated with red. The level 1 low velocity impact has an energy of 25J, the level 2 impact has 50J energy.

The C72 frame sub-model analyses are considered here only for the LBL limit load case on the level of panel DFEM, for which the load identification procedure was previously described. For these loads as determined from the load identification procedure, the responses are determined for the whole panel DFEM, and in much more detail in the frame sub-model. The frame is represented by continuum shell elements (SC8R) in both the DFEM and the sub-model, but the mesh size in the frame is decreased from approximately 25mm in the DFEM to approximately 3mm in the sub-model. Figure 10 shows the principal strains plots in both the DFEM and the sub-model. It can be seen that the strains in both models are consistent, as expected.

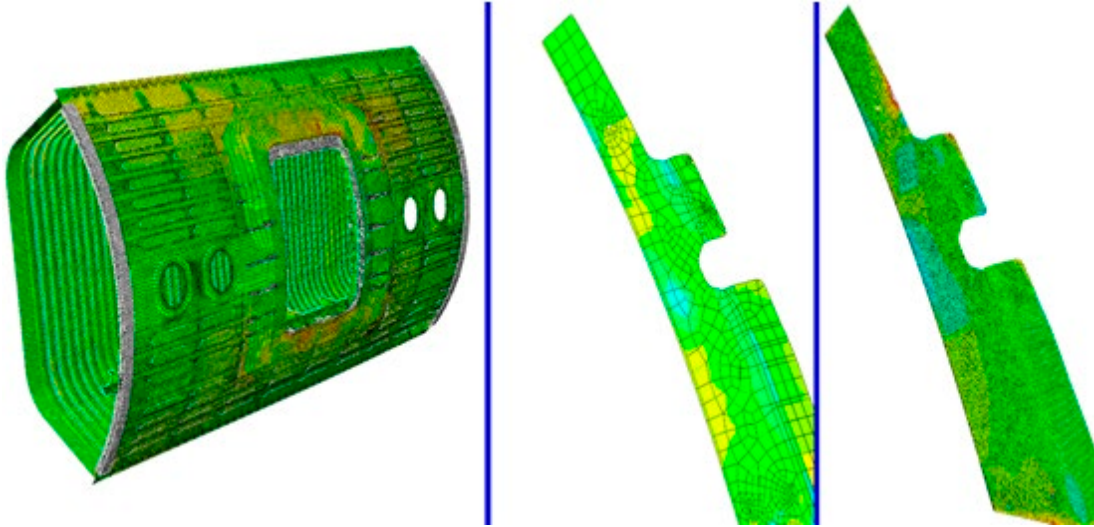


Figure 10 Panel DFEM (left) with principal strains plots and the original C72 frame part with coarse mesh (middle) and the C72 frame upper-part sub-model with fine mesh (right).

7. Damage analyses

This paper now focusses on an impact damage evaluation study for the LBL load case using sub-model analyses on a composite frame corner near the door section (C72 frame, Figure 9). This frame component is quite exposed and therefore susceptible for impact during assembly or in-service. Therefore a local damage analysis model is made with a simplified L-profile geometry that corresponds to the frame corner geometry. This damage analysis model has a ply-by-ply local composite laminate representation (modelled including damage and failure mechanics; lamina material properties are based on HexPly® M21E/IMA carbon fibre/epoxy prepreg) to also include delamination damage between all layers, see Figure 12. With this damage analysis model the local impact damage on the frame corner is evaluated. The damaged area is then incorporated in the sub-model of the doorframe on which the global displacements coming from the side panel DFEM are transposed to determine if residual strength of the frame is sufficient.

The composite damage model that is used, is based on damage mechanics for plane stress which means that damage evolution will result in stiffness reduction of the lamina material. This is commonly performed by introducing a damage parameter e.g. d_1 , d_2 depending on the damage mode (transverse crack, fibre damage) in the element stiffness matrix, see equation 3. The out of plane damage behaviour is described by the cohesive interaction method discussed below.

$$\begin{pmatrix} \varepsilon_{11} \\ \varepsilon_{22} \\ \varepsilon_{12}^{nl} \end{pmatrix} = \begin{pmatrix} \frac{1}{(1-d_1)E_1} & \frac{-\nu_{12}}{E_1} & 0 \\ \frac{-\nu_{21}}{E_2} & \frac{1}{(1-d_2)E_2} & 0 \\ 0 & 0 & \frac{1}{(1-d_{12})2G_{12}} \end{pmatrix} \begin{pmatrix} \sigma_{11} \\ \sigma_{22} \\ \sigma_{12} \end{pmatrix} \quad (3)$$

Cohesive interaction is based on well-established traction separation laws that describe the relative displacement Δ of two connected surfaces and depending on the element stiffness determine the internal traction. The interface damage modes that are assumed are Mode I (peel), and Mode II, III (shear), see Figure 11. The approach allows a linear softening of the interface when the damage is initiated.

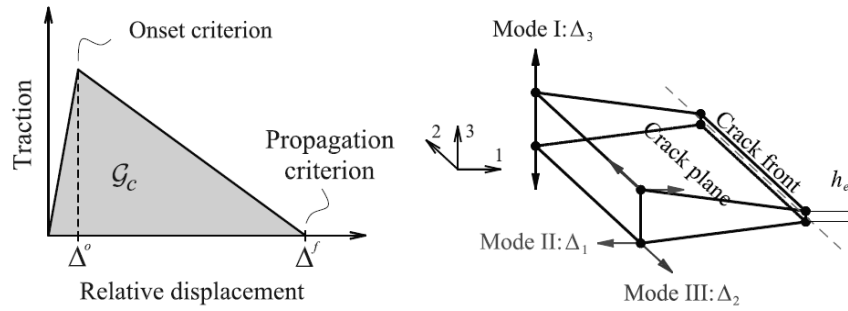


Figure 11 Traction separation graph depending on the relative displacement of the two connection surfaces and the mode discrimination in the cohesive model [9].

The inputs needed for the cohesive surfaces are the strength values for the damage initiation of the interface and the fracture toughness G_{Ic} , G_{IIc} , G_{IIIc} for the three modes. The interaction between the modes is determined using the Benzeggagh-Kenane (BK) [10] mixed mode law shown in equation 4.

$$G_c = G_{Ic} + (G_{IIc} - G_{Ic}) \frac{G_{II} + G_{III}}{G_I + G_{II} + G_{III}}^\alpha \tag{4}$$

Where G_c is the total mixed mode fracture energy, G_{Ic} , G_{IIc} , G_{IIIc} the critical fracture toughness energy and G_I , G_{II} , G_{III} the fracture toughness values during the simulation. The critical fracture toughness values are determined experimentally with double cantilever beam (DCB) or end notched flexure (ENF) testing. The combination of the damage mechanics and failure mechanics methods allow for simulation of the common damage modes in composites, such as matrix cracking, fibre failure and delaminations. In the next section the use of these methods will be described on the door frame impact use-case. The door frame section and detailed 24 layer ply-by-ply composite model in the radius of the door frame is shown in Figure 12. The ply-by-ply composite model is supported at the curved sides and loaded by the rigid impactor body.

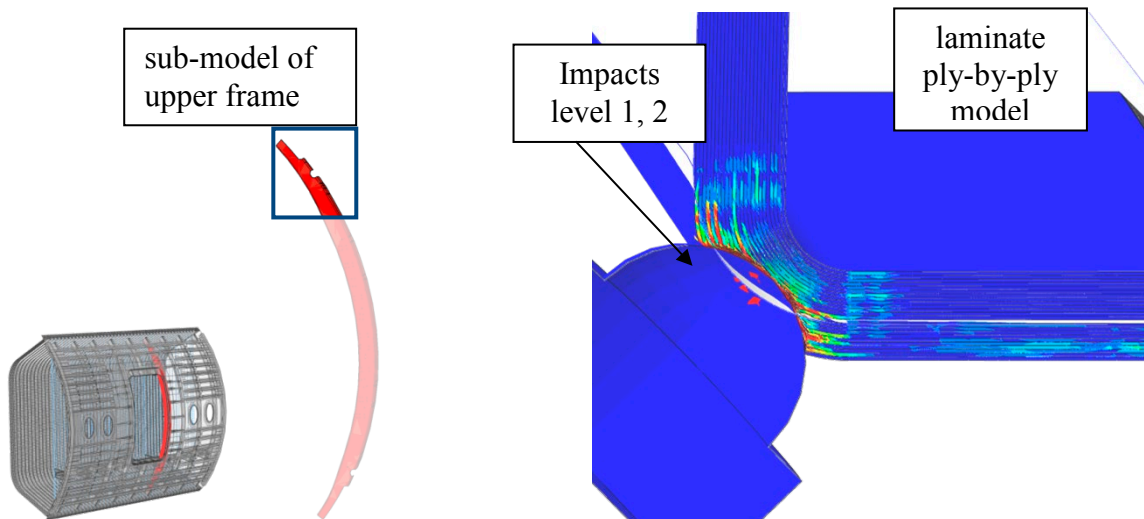


Figure 12 Frame section sub-model of the upper frame part (left) and the ply-by-ply composite model (right) for damage analysis of the frame corner and steel impactor (blue) to evaluate the ply damage and delamination from the 25J and 50J impacts.

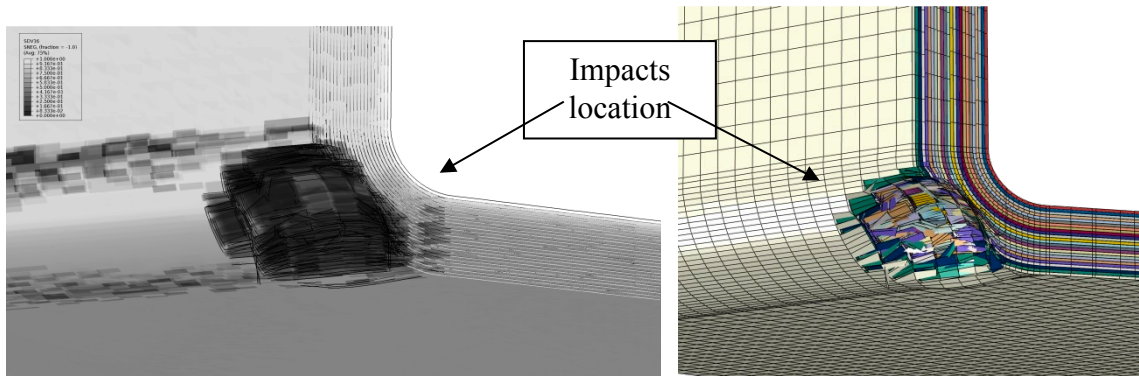


Figure 13 Damage levels after the 25J impact in the composite laminate. The black elements indicate damage. At the impact location, clearly, a large proportion of the laminate’s plies are damaged.

The sub-model for this case is the C72 door frame structure, to which intercostal structures, door hinges and doorstops are connected. In the damage analysis model the low velocity impact is modelled with 25J impact energy and a 16mm radius rigid sphere impactor with a mass of 2 kg, 5 m/s velocity, resulting in a near BVID damage. The level 2 impact damage is obtained here from a 50J, 7.07m/s velocity, impact event. The model contains 283k continuum shell elements and uses surface cohesive definitions (23 interfaces). The resulting damage from an impact on the corner is significant as can be observed in the Figure 12 and Figure 13. This location proved to give the most damage in a relative high strain area of the frame component. Some de-laminations can be observed and the impactor is almost protruding the laminate. For the 50J impact similar damage behaviour is observed, only a larger area is damaged.

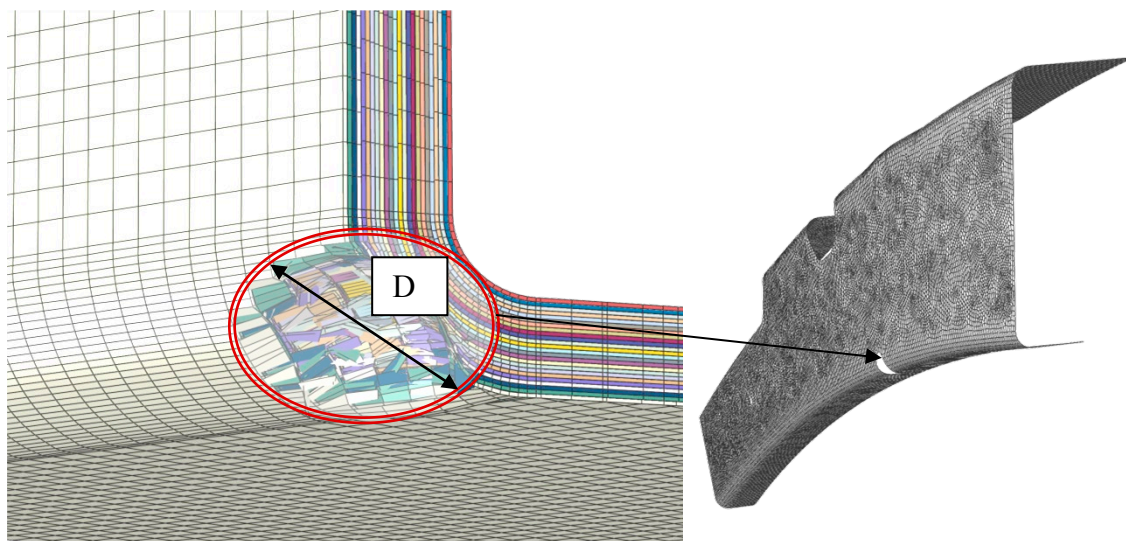


Figure 14 Indicative size (D) for the damaged laminate in the corner of the frame using the *soft-inclusion* approach, Nilsson [9]. On the right the damaged frame sub-model with the *soft-inclusion* region as derived from the laminate level.

This resulting impact damage is represented in the frame sub-model as a *soft-inclusion* region (homogenization, as also investigated by Nilsson [9]) to assess the residual strength of the frame in the panel. From the impact simulation results it was observed that the influence region by the impact is circular and has a diameter of 20 mm for the 25J impact and 32mm for the 50J impact. The de-laminations are represented in this *soft-inclusion* region but not explicitly included in the sub-model, see Figure 14. The highest strain level occurs near the load introduction with levels of around 2000 micro-strain.

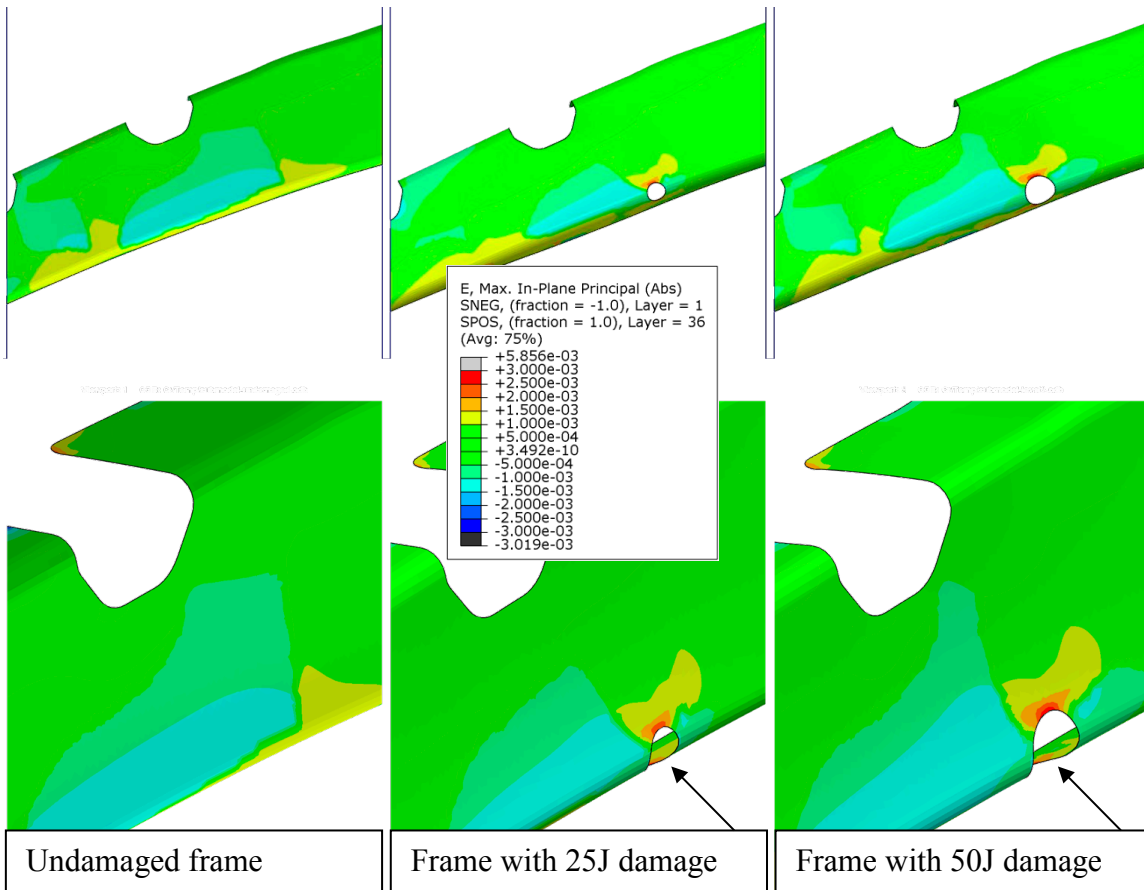


Figure 15 Frame sub-model strain results for the un-damaged frame (on the left) and with the *soft-inclusion* regions due to the 25J (middle) and 50J (on the right) impact damages in the corner area. For visualization the *soft-inclusion* elements are removed. Near the *soft-inclusion* regions, the increase in local strain can be clearly observed.

From the results of the sub-model of the impact-affected region it may be concluded that there is a significant influence of a low velocity impact on the strength of the component. The local strain value for the un-damaged region is found to be about 2000 micro-strain, but increases up to about 5000 micro-strain locally around the impact damage (Figure 15). From previous experiments on impacted samples of carbon/epoxy prepreg laminates it is expected that damages resulting in such strain value will remain stable during static and fatigue loading during the test campaign (virtual assessment of no-growth principle). However more research has to be done on the delamination growth effect since this is not included in the sub-model. Higher impact energies above 50J are likely to result in damage growth.

8. Global conclusions and discussion

An investigation for an innovative large panel test procedure is presented. The focus of this study is not on the development of the actual physical test procedure, but it aims to support the development of the innovative physical test set-up through detailed modelling of the test-sample including the relevant aspects of the test-rig. In particular a virtual testing study is described of a large composite fuselage side panel with substantial structural details like floor beams, window frames and PAX door. Proper load introductions and boundary conditions from the test rig are incorporated and the global structural response is evaluated. An identification study is presented using the barrel and panel strains for the proper determination of the load values to be applied in the physical test procedure. The local structural response in a frame sub-component is evaluated in high detail using ABAQUS sub-modelling in order to accurately capture the strain state in the test and to identify possibly local failures in the component.

The sub-modelling approach has been used to evaluate in high detail the localised region around damage locations. Various levels of damage modelling have been applied for accurate prediction of progression from inflicted category 1 and 2 impact damages. It has been demonstrated that these damages can be expected to remain stable during the test campaign (virtual assessment of no-growth principle). This small sub-modelling study was mainly intended to

illustrate the applicability of this approach for detailed assessment of local artefacts in the tests, which may be related to impact or manufacturing damages or local repairs.

The sub-model approach has shown to efficiently refine local component models (in this case for a composite fuselage frame) for damage assessment taking global loading conditions (in this case for a composite fuselage panel test) into account. A downside of this one-way global-local coupling from the global model to the local model is that no load re-distribution in the global model due to stiffness changes will occur. For instance the impact damage might reduce the overall stiffness of the frame component, while this reduced frame stiffness is not updated in the global model frame component. For small local damages this approach may be assumed valid, but for larger more significant cracks in such components a two-way global-local-global coupling should be used.

References

- [1] Bakuckas, J.G. Jr., C.A. Bigelow and P.W. Tan, "The FAA Full-Scale Aircraft Structural Test Evaluation and Research (FASTER) Facility," Proceedings from the International Workshop on Technical Elements for Aviation Safety, Tokyo, Japan, pp. 158-170, 1999.
- [2] IMA Materialforschung und Anwendungstechnik GmbH, http://www.ima-dresden.de/index.php?ILNK=bauteilpruefung_luftfahrt_flugzeugrumpfschalen&iL=2 (last accessed 8-10-2014).
- [3] <http://blog.flightstory.net/630/787-completes-fuselage-barrel-test/> (last accessed 12-3-2015).
- [4] Ostergaard, M.G., A.R. Ibbotson, O. Le Roux and A.M. Prior, Virtual testing of aircraft structures, CEAS Aeronaut J, 1:83–103, 2011.
- [5] Dassault Systèmes, CATIA product page, <http://www.3ds.com/products-services/catia/> (last accessed 12-3-2015).
- [6] Dassault Systèmes, ABAQUS product page, <http://www.3ds.com/products-services/simulia/products/abaqus/> (last accessed 12-3-2015).
- [7] U.S. Department of Transportation, Federal Aviation Administration, ‘Composite aircraft structure’, Advisory Circular AC No: 20-107B, Change 1, 24 August 2010.
- [8] MAAXIMUS project, www.maaximus.eu (last accessed 12-3-2015).
- [9] Nilsson, E. 2005. Residual strength prediction of composite laminates containing impact damage, Master Thesis, Linköping University, Sweden.
- [10] Benzeggagh, M. L. and M. Kenane. 1996. Measurement of Mixed-Mode Delamination Fracture Toughness of Unidirectional Glass/Epoxy Composites with Mixed-Mode Bending Apparatus, *Composites Science and Technology*, vol. 56, pp. 439–449, 1996.

Acknowledgements

The research leading to these results has received funding from the European Community’s Seventh Framework Programme FP7/2007-2013 under grant agreement n°213371 (MAAXIMUS, www.maaximus.eu).